Supplemental material submitted for the paper

The importance of ocean transport in the fate of anthropogenic CO_2

L. Cao, M. Eby, A. Ridgwell, K. Caldeira, D. Archer, A. Ishida, F. Joos, K. Matsumoto, U. Mikolajewicz, A. Mouchet, J. C. Orr, G.-K. Plattner, R. Schlitzer, K. Tokos, I. Totterdell, T. Tschumi, Y. Yamanaka , A. Yool

Introduction:

This supplemental material includes one table and two figures. Table S1 compares parameter values used in three versions of the GENIE-1 model. Figure S1 shows the effect of vertical diffusivity, vertical resolution, and seasonality on modeled oceanic uptake of anthropogenic CO_2. Figure S2 shows the effect of marine biology on modeled oceanic uptake of anthropogenic CO_2.

Table S1. Controlling parameters in different versions of the GENIE-1 model.

Parameter Name	**GENIE8**	**GENIE16**	**MESMO**	**Parameter description and units**
Ocean physics [a]				
W	1.93	1.531	2.208	Wind-scale
κ_h	4489	1494	4467	Isopycnal diffusion (m^2 s^{-1})
κ_v	0.27	0.25	0.1 to1.2	Diapycnal diffusion (cm^2 s^{-1})
λ	2.94	2.71	2.21	1/friction (days)
Atmosphere physics [a]				
k_T	4.67×10^6	5.20×10^6	3.27×10^6	T diffusion amplitude (m^2 s^{-1})
l_d	1.08	1.41	0.979	T diffusion width (Radians)
s_d	0.06	0.09	0.1700	T diffusion slope
κ_q	1.10×10^6	1.17×10^6	1.70×10^6	Q diffusion (m^2 s^{-1})
β_T	0.11	0.0010	0.0023	T advection coefficient
β_q	0.23	0.165	0.23	Q diffusion coefficient
F_a	0.23	0.73	0.36	FW flux factor (Sv)
Sea-ice physics [a]				
κ_{hi}	6200	3574	5579	Sea-ice diffusion (m^2 s^{-1})
Ocean biogeochemistry [b]				
$u_0^{PO_4}$	1.96	8.99	1.91	maximum PO_4 uptake rate (μmol kg-1 yr^{-1})
K^{PO_4}	0.22	0.89	0.21	PO_4 half-saturation concentration (μmol kg^{-1})
r^{POC}	0.065	0.056	0.055	partitioning of POC export into fraction #2
l^{POC}	550	590	*variable*	*e*-folding depth of POC fraction #1 (m)
l_2^{POC}	∞	∞	∞	*e*-folding depth of POC fraction #2 (m)
$r_0^{CaCO_3:POC}$	0.044	0.048	0.046	$CaCO_3$:POC export 'rain ratio' scalar [c]
η	0.81	0.77	1.28	calcification rate power
r^{CaCO_3}	0. 4325 [d]	0.45 [d]	0.49	partitioning of $CaCO_3$ export into fraction #2
l^{CaCO_3}	1083	1890	*variable*	*e*-folding depth of $CaCO_3$ fraction #1 (m)
$l_2^{CaCO_3}$	∞	∞	∞	*e*-folding depth of $CaCO_3$ fraction #2 (m)

[a] See: Edwards and Marsh (2005); Hargreaves et al. (2004); Ridgwell et al. (2007a); Singarayer et al. (2008), Matsumoto (2008)

[b] See: Ridgwell et al. (2007a,b); Ridgwell and Hargreaves (2007).

[c] Note that the rain ratio scalar parameter is not the same as the actual $CaCO_3$:POC export rain ratio because it is multiplied by $(\Omega - 1)^\eta$ where Ω is the surface ocean saturation state (with respect to calcite), as described in Ridgwell et al. (2007a,b). Pre-industrial mean ocean surface Ω is ~5.2 in the GENIE-1 model, so that the global $CaCO_3$:POC export rain ratio can be estimated using the 8-parameter assimilation [d] as being equal to $(5.2 - 1)^{0.81} \times 0.044 = 0.14$.

[d] Adjusted compared to formal calibration in order to achieve an improved prediction of mean sediment surface wt% $CaCO_3$ compared to observations (Ridgwell and Hargreaves, 2007).

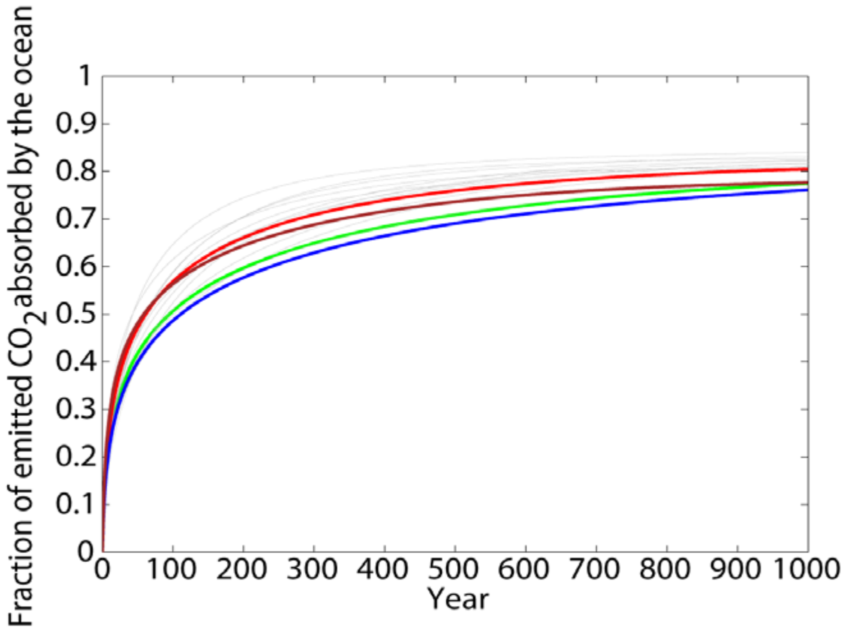

Fig. S1 Model-simulated oceanic uptake of CO_2 in response to a CO_2 pulse emission of 590.2 PgC (corresponding to an instantaneous doubling of atmospheric CO_2 from 278 to 556 ppm). Results from different runs using the GENE16 model are shown: GENIE16 base run as shown in Fig. 1(green), GENIE16 run with vertical diffusivity doubled from 0.25 to 0.5 $cm^{-2}\ s^{-1}$ (red), GENIE16 run with vertical resolution reduced from 16 to 8 levels (brown), GENIE16 run with the seasonal cycle removed (blue). Other model results as shown in Fig. 1 are presented here in grey lines.

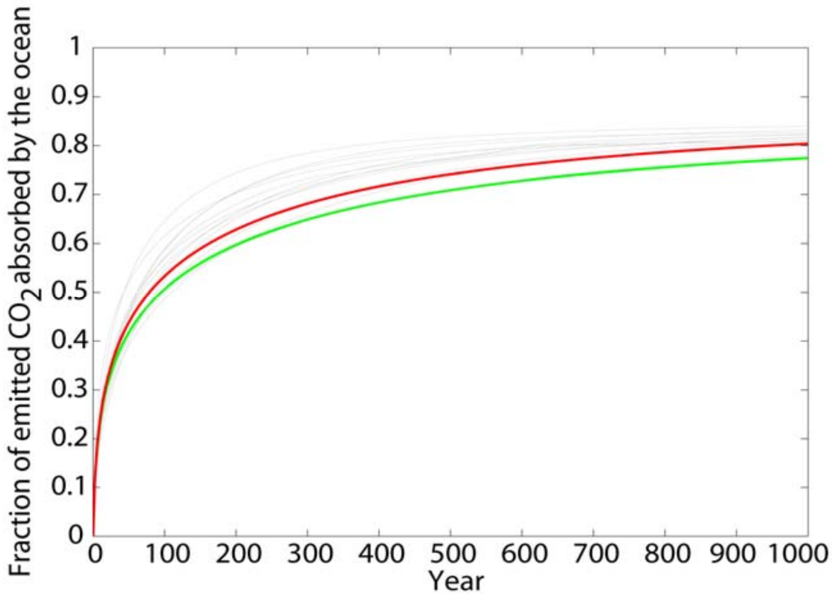

Fig. S2 Model-simulated oceanic uptake of CO_2 in response to a CO_2 pulse emission of 590.2 PgC (corresponding to an instantaneous doubling of atmospheric CO_2 from 278 to 556 ppm). Results from two different runs using the GENE16 model are shown: GENIE16 base run as shown in Fig. 1 (green), GENIE16 run without the inclusion of marine biology (red). Other model results as shown in Fig. 1 are presented here in grey lines. The abiotic run absorbs more excess CO_2 than the biotic run because during model spinup the removal of marine biology leads to higher surface alkalinity (a global mean value of 2361.9 µmole/kg in abiotic run compared with 2271.5 µmole/kg in biotic run). Higher surface alkalinity leads to greater buffering capacity of the ocean to absorb excess CO_2.

References:

Edwards, N. R., and R. Marsh, Uncertainties due to transport-parameter sensitivity in an efficient 3-D ocean-climate model, Climate Dynamics, 24 (4) 415 – 433, 2005.

Hargreaves, J. C., J. D. Annan, N. R. Edwards, R. Marsh, An efficient climate forecasting method using an intermediate complexity Earth System Model and the ensemble Kalman filter, Climate Dynamics, 23 (7-8), 745 – 760, 2004.

Matsumoto, K. S. Tokos, A. Price, and S. J. Cox, First description of the Minnesota Earth System Model for Ocean biogeochemistry (MESMO 1.0), Geoscientific Model Development, 1, 1-15, 2008.

Ridgwell, A., and J. C. Hargreaves, Regulation of atmospheric CO_2 by deep-sea sediments in an Earth system model, Global Biogeochem. Cycles, 21, GB2008, doi:10.1029/2006GB002764, 2007.

Ridgwell, A., I. Zondervan, J. Hargreaves, J. Bijma, and T. Lenton, Assessing the potential long-term increase of oceanic fossil fuel CO_2 uptake due to 'CO_2-calcification feedback', Biogeosciences 4, 481-492, 2007a.

Ridgwell, A., J. Hargreaves, N. Edwards, J. Annan, T. Lenton, R. Marsh, A. Yool, and A. Watson, Marine geochemical data assimilation in an efficient Earth System Model of global biogeochemical cycling, Biogeosciences 4, 87-104, 2007b.

Singarayer J. S., D. A. Richards, A. Ridgwell, P. J. Valdes, W. E. N. Austin, J. W. Beck, An oceanic origin for the increase of atmospheric radiocarbon during the Younger Dryas, Geophys. Res. Lett. 35, L14707, doi:10.1029/2008GL034074, 2008.